J Fluoresc (2015) 25:1655–1661
DOI 10.1007/s10895-015-1652-8

ORIGINAL ARTICLE

Influence of the Ring Size on the Binding Ability of FTO Investigated by Fluorescence Spectroscopy

Wu He[1] · Zhigang Li[1] · Lingling Yang[1] · Qingwei Jiang[1] · Ting Ren[1] · Lijiao Zhang[1] · Zhenhua Shen[1] · Qinghua Yang[1] · Ruiyong Wang[1] · Junbiao Chang[1]

Received: 29 May 2015 / Accepted: 9 September 2015 / Published online: 16 September 2015

Abstract The fat mass and obesity associated protein (FTO) is a potential target for anti-obesity medicines. In this paper, we have synthesized two potential inhibitors for FTO, three-member-ring compound ($\mathbf{W_3}$) and four-member-ring compound ($\mathbf{W_4}$). The interactions of fat mass and obesity-associated (FTO) protein with $\mathbf{W_3}$ (or $\mathbf{W_4}$) have been studied by spectral method. Results show the intrinsic fluorescence is quenched by the $\mathbf{W_3}$ (or $\mathbf{W_4}$). The thermodynamics parameters indicate hydrophobic interaction play a major role in the interactions. The results of synchronous fluorescence spectra demonstrate that the microenvironments of Trp residue of FTO are disturbed by $\mathbf{W_3}$ and $\mathbf{W_4}$. Results showed that $\mathbf{W_3}$ are stronger quenchers and bind to FTO with the higher affinity than $\mathbf{W_4}$. The influence of molecular structure on the binding aspects has been investigated.

Keywords FTO · Four-member-ring compound · Three-member-ring compound · Fluorescence · Binding

Introduction

The fat mass and obesity-associated (FTO) gene was placed center stage when common intronic variants within the gene were robustly associated with human obesity. FTO protein has been demonstrated to influence human obesity and energy utilization in up to half the world's population. Murine models of perturbed FTO expression have shown effects on body weight and composition [1]. FTO protein, belonging to the Fe(II) and 2-oxoglutarate (2OG)-dependent oxygenase family, is an N-methyl nucleic acid demethylase acting on both single-stranded DNA and RNA substrates. In addition, it is reported that FTO involved in various disease, such as obesity, cardiovascular diseases, type II diabetes, heart disease and so on [2–4]. The recently reported crystal structure of FTO has offered insights into cofactors and substrate binding sites. Taken together with the extensive structural and mechanistic studies of AlkB family proteins, these studies enable the rational design and development of inhibitors targeting RNA demethylases [2]. There is an unmet medical need for new approaches to treating obesity. How the modulation of nucleic acid methylation status by FTO relates to increased body mass has remained elusive. Possible mechanisms and potential FTO inhibitors have been reported recently [3, 4].

Three-member-ring compounds ($\mathbf{W_3}$) and four-member-ring compounds ($\mathbf{W_4}$) has been obtained in our lab as shown in Fig. 1. Recently our experimental results indicate that $\mathbf{W_4}$ may be potential inhibitors for FTO [5].

Drug-protein interaction may also have an influence on the structure of the protein. Thus, the study on the interactions of ligands with proteins is important in understanding the action of these molecules in the body [6]. The nature and magnitude of drug-protein interaction significantly influences the biological activity of the drug. Several analytical methods have been used to qualitatively and quantitatively study the binding of ligands to protein [7–11]. Fluorescence techniques are great aids in the study of interactions between drugs and proteins because of the high sensitivity,

Wu He and Zhigang Li contributed equally to this work.

✉ Ruiyong Wang
wangry@zzu.edu.cn

✉ Junbiao Chang
changjunbiao@zzu.edu.cn

[1] College of Chemistry and Molecular Engineering, Zhengzhou University, 100 Science Avenue, Zhengzhou 450001, People's Republic of China

rapidity, and ease of implementation. The techniques both offer qualitative insight into interactions and provide estimated binding constants that agree with those obtained by established methods [12].

FTO contains tyrosine (Tyr) and tryptophan (Trp) residues [4, 13]. The presence of tryptophan residues offers an advantage to studying the ligand binding process using fluorescence spectroscopy [14]. The interactions between drugs and protein can been studied by fluorescence spectroscopy [15–19]. Therefore, the association behaviors between the synthesized compounds ($\mathbf{W_3}$ and $\mathbf{W_4}$) and FTO were investigated by spectroflourimetric method for the first time.

In the present study, the association behaviors between FTO and $\mathbf{W_3}$ (or $\mathbf{W_4}$) were investigated by spectroscopic methods. An important aspect of this study was to gain insight into the structural changes of FTO induced allosterically by $\mathbf{W_3}$ (or $\mathbf{W_4}$) binding. The microenvironments of Trp residue of FTO were disturbed by $\mathbf{W_3}$ (or $\mathbf{W_4}$). These results will be helpful in understanding the interactions between FTO and the synthesized compounds.

Experimental Section

Materials

FTO were provided from Prof. Jijie Chai (Tsinghua University). FTO stock solutions were prepared in 10 mM Tris–HCl buffer, pH 7.4. All chemicals were of analytical grade and were used without further purification. Double distilled water was used throughout the experiment. $\mathbf{W_3}$ and $\mathbf{W_4}$ were synthesized in our lab [5], and their molecular structures were shown in Fig. 1. Stock solutions (4.0×10^{-3} M) were prepared in ethanol.

Apparatus

Absorption spectra were acquired in an Agilent 8453 UV-visible spectrophotometer. Steady-state fuorescence spectra were acquired on a F-4600 spectrofuorometer (HITACHI, Japan). The pH values were measured by a pH-3 digital pH-meter (Lei Ci, Shanghai) with a combined glass electrode. For steady-state fuorescence spectra experiments, the excitation wavelength was 285 nm, and the emission was monitored from 295 to 500 nm (1 nm increments). The excitation and emission monochromator slit widths were 5 nm and were held constant during all experiment.

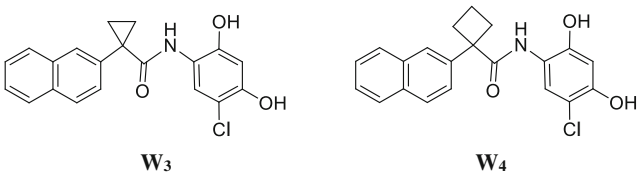

$\mathbf{W_3}$ $\mathbf{W_4}$

Fig. 1 The molecular structures of $\mathbf{W_3}$ and $\mathbf{W_4}$

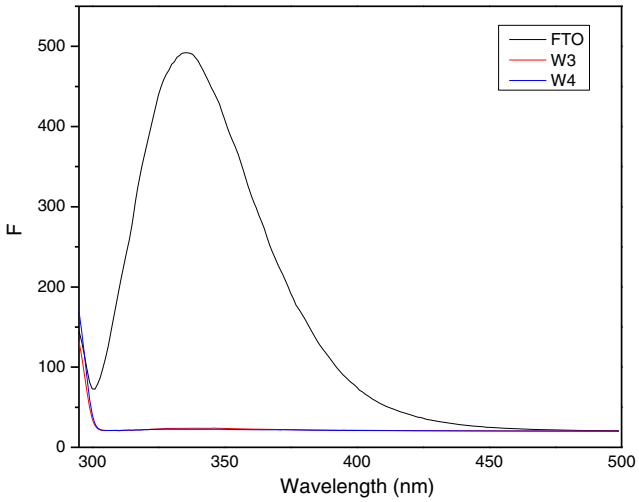

Fig. 2 The fluorescence spectra of FTO (1.5×10^{-5} M), W_3 (2.0×10^{-4} M) and W_4 (2.0×10^{-4} M) in 10 mM Tris–HCl pH=7.40. W_3 and W_4 do not show any appreciable fluorescence at an excitation wavelength of 285 nm

Spectroflourimetric Experiments

In experiments, FTO concentration was fixed at 15 μM while varying $\mathbf{W_3}$ (or $\mathbf{W_4}$) concentrations in the range of 10.0–230.0 μM in a total volume of 3.0 mL. After an incubation of 10 min in water bath, fluorescence spectra were recorded in the same way as described above. To study the effect of temperature on the $\mathbf{W_3}$ (or $\mathbf{W_4}$)−FTO interaction, experiments were carried out at three different temperatures, viz. 16 °C, 27 °C and 35 °C. The fluorescence intensity was recorded after an equilibration of 10 min at each temperature.

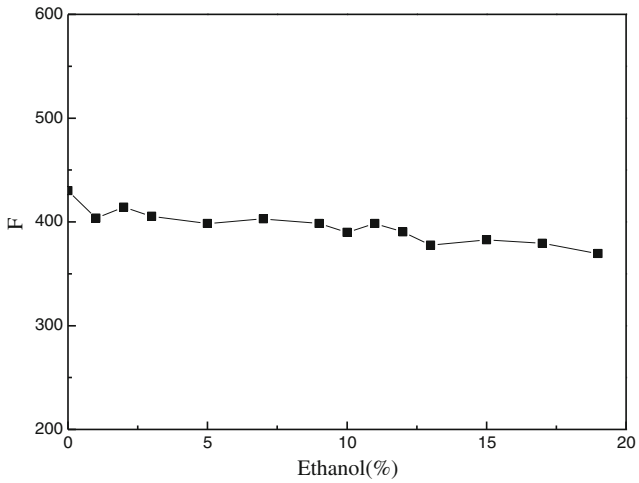

Fig. 3 The influence of ethanol on the FTO fluorescence in 10 mM Tris–HCl pH=7.40 at an excitation wavelength of 285 nm. FTO solution was mixed with ethanol instead of $\mathbf{W_3}$ (or $\mathbf{W_4}$)

Synchronous fluorescence spectra of the protein samples were obtained in the wavelength range of 260–360 nm and 280–400 nm for the difference between excitation and emission wavelengths (Δλ) of 15 and 60 nm, respectively.

Results and Discussion

Fluorescence Spectra of W_3 and W_4

The fluorescence spectra of W_3, W_4 and FTO were shown in Fig. 2. The solution of W_3 and W_4 were nonfluorescence. FTO exhibited strong fluorescence excited at 285 nm. So the interaction between FTO and W_3 (or W_4) can be investigated from the fluorescence change.

Influence of Ethanol on Fluorescence

W_3 and W_4 was dissolved in ethanol. The influence of ethanol on the FTO fluorescence was shown in Fig. 3. Results indicated little effect was caused by the addition of ethanol. So the fluorescence change in the interaction of FTO with W_3 (or W_4) was caused by the addition of W_3 (or W_4). Our previous studies also indicated that the small amount of ethanol did not influence the fluorescence of albumin [20].

Fluorescence Quenching Measurements

Binding resulted in a decrease in fluorescence intensity for W_3 and W_4. Figure 4 showed representative data for W_3 and W_4 binding to FTO. At W_3 (or W_4): FTO mole ratios (as high as 15:1), $\lambda_{EM,max}$ remains almost constant for W_3 and W_4. No obvious shift was observed at the maximum emission wavelength.

Qualitative observations showed that the conformational changes occurred upon W_3 (or W_4) binding to FTO, as well as the fluorescence data may also be quantified to estimate

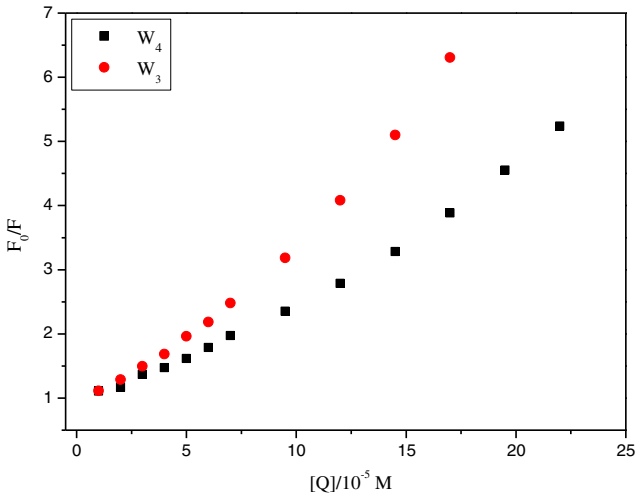

Fig. 5 Data were fit by Stern-Volmer equation at 27 °C. The fluorescence of FTO was quenched by W_3 (or W_4) in 10 mM Tris–HCl pH=7.40 at an excitation wavelength of 285 nm. The concentration of W_3 (or W_4) and FTO are the same as those in Fig. 4

association constants for the FTO–W_3 (or W_4) complexes. The fluorescence data were analyzed using the Stern-Volmer equation as shown in Fig. 5 [21]:

$$\frac{Fo}{F} = 1 + K_q\tau_0[Q] = 1 + K_{sv}[Q] \quad (1)$$

Where, F_0 and F are the fluorescence intensities of FTO in the absence and presence of the quencher, respectively; K_{sv} is the Stern-Volmer quenching constant; K_q is the diffusion-controlled quenching rate constant; τ_0 is the average lifetime of the biomolecule without quencher ($\tau_0 \approx 10^{-8}$ s) [22]; [Q] is the concentration of W_3 (or W_4).

For clear comparison between W_3 and W_4 in the same graph, data fit by Stern-Volmer equation at 27 °C was show Fig. 5. Table 1 and Fig. 6 showed representative data fit by Stern-Volmer equation at 16, 27 and 35 °C. It was found that

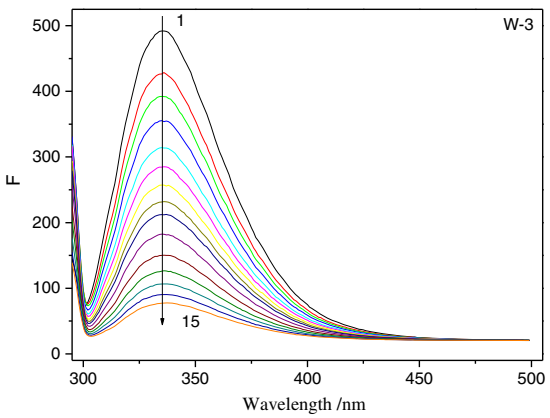

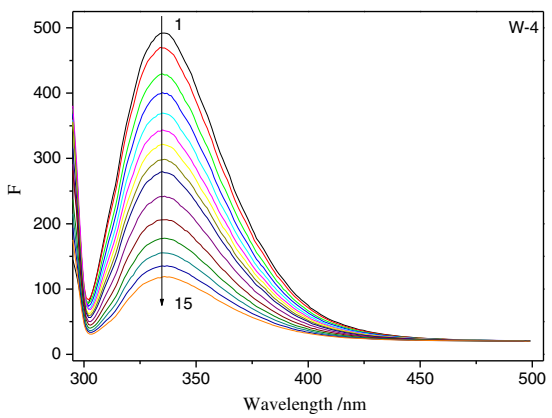

Fig. 4 FTO fluorescence decreases upon titration with W_3 or W_4 in 10 mM Tris–HCl pH=7.40 at an excitation wavelength of 285 nm. The concentration of FTO is 1.5×10^{-5} mol L^{-1}. The concentration of W_3 (or W_4) is 0, 1.0×10^{-5}, 2.0×10^{-5}, 3.0×10^{-5}, 4.0×10^{-5}, 5.0×10^{-5}, 6.0×10^{-5}, 7.0×10^{-5}, 8.0×10^{-5}, 1.0×10^{-4}, 1.3×10^{-4}, 1.5×10^{-4}, 1.8×10^{-4}, 2.0×10^{-4} and 2.3×10^{-4} mol L^{-1} respectively (From *top* to *bottom*)

Table 1 The quenching constants ($L \cdot mol^{-1} \cdot S^{-1}$) between W_3 (or W_4) and FTO by Stern-Volmer equation

Complex	T(°C)	Stern-Volmer equation	Kq($L \cdot mol^{-1} \cdot S^{1}$)	R
W_4	16	$F_0/F=0.9716+0.1127\times10^5[Q]$	1.1270×10^{12}	0.9990
W_3	16	$F_0/F=0.4832+0.2328\times10^5[Q]$	2.3276×10^{12}	0.9993
W_4	27	$F_0/F=0.6816+0.1880\times10^5[Q]$	1.8799×10^{12}	0.9997
W_3	27	$F_0/F=0.7249+0.2473\times10^5[Q]$	2.4733×10^{12}	0.9978
W_4	35	$F_0/F=0.5367+0.2858\times10^5[Q]$	2.8583×10^{12}	0.9990
W_3	35	$F_0/F=0.3292+0.4133\times10^5[Q]$	4.1333×10^{12}	0.9987

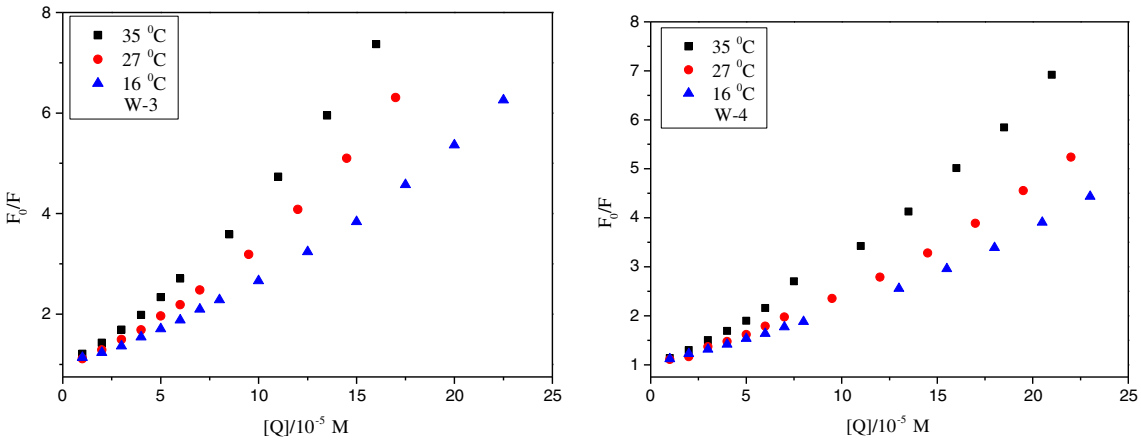

Fig. 6 Data were fit by Stern-Volmer equation at 16, 27 and 35 °C. The fluorescence of FTO was quenched by **W_3** (or **W_4**) in 10 mM Tris–HCl pH= 7.40 at an excitation wavelength of 285 nm. The concentration of W_3 (or W_4) and FTO are the same as those in Fig. 4

the graphs in Figs. 5 and 6 were non-linear when the concentration of **W_3** (or **W_4**) was high than 1.0×10^{-4} mol L^{-1}. The plot of (F_0/F) against concentration of quencher [Q] was observed straight line in the range of 1.0–8.0$\times10^{-5}$ mol L^{-1}. In order to obtain K_{sv} from slopes, the plot in the concentration range of 1.0–8.0$\times10^{-5}$ mol L^{-1} for **W_3** (or **W_4**) was used. The K_q can be obtained based on $K_{sv}=K_q\tau_0$. Values of K_q were obtained from the slope of these plots based on Eq. (1) and were listed in Table 1.

As can be seen from the results in Figs. 5, 6 and Table 1, K_q is temperature dependent and a positive correlation between K_q and temperature was noticed. Static quenching is characterized by the decrease in the quenching constant with the increase in temperature [23]. The K_q in Table 1 was the order of 10^{12} $L \cdot mol^{-1} \cdot S^{-1}$, which was greater than the maximum scatter collision quenching constant of various quenchers. Larger K_q values obtained for the FTO–**W_3** (or **W_4**) system compared to the highest value reported for a diffusion-controlled process (2.0×10^{10} $L \cdot mol^{-1} \cdot S^{-1}$) also opposed the involvement of dynamic quenching in the binding process [23]. According to the conclusions in the references [24, 25], these results suggested that the quenching of FTO fluorescence by **W_3** (or **W_4**) was due to the formation of a complex.

Analysis of Binding Equilibria

Assuming the binding of **W_3** (or **W_4**) as independent to a set of equivalent sites on FTO, the binding constants (K_a) and binding sites (n) can be calculated by the following double-logarithm equation based on Eq. (2) [26].

Table 2 The binding constants ($L \cdot mol^{-1}$) between W_3 (or W_4) and FTO

Complex	T(°C)	Double-logarithm equation	Ka($L \cdot mol^{-1}$)	R	n
W_4	16	$\log(F_0-F)/F=4.6968+1.1568\log[Q]$	4.9750×10^4	0.9994	1.1568
W_3	16	$\log(F_0-F)/F=5.3769+1.2854\log[Q]$	2.3819×10^5	0.9996	1.2854
W_4	27	$\log(F_0-F)/F=4.8682+1.1722\log[Q]$	7.3841×10^4	0.9982	1.1722
W_3	27	$\log(F_0-F)/F=5.7576+1.3426\log[Q]$	5.7227×10^5	0.9996	1.3426
W_4	35	$\log(F_0-F)/F=5.1877+1.2136\log[Q]$	1.5405×10^5	0.9996	1.2136
W_3	35	$\log(F_0-F)/F=5.8523+1.3326\log[Q]$	7.1164×10^5	0.9994	1.3326

Table 3 Thermodynamic parameters of interaction between W_3 (or W_4) and FTO

Complex	T (°C)	ΔG (J·mol^{-1})	ΔH (J·mol^{-1})	ΔS (J·mol^{-1} ·K^{-1})
W_3	15	-2.1402×10^4	1.6470×10^4	131.50
W_4	15	-2.3983×10^4	3.0512×10^4	189.22
W_3	27	-2.2980×10^4		
W_4	27	-2.6254×10^4		

$$\log\frac{F_0-F}{F} = \log K_a + n\log[Q] \quad (2)$$

Plots of log ((F_0-F)/F) versus log[Q] for FTO−**W_3** (or **W_4**), which were shown in Table 2, listed the corresponding calculated results with all the correlation coefficient over 0.99. The values of binding constants of **W_3** (or **W_4**) to FTO were in the range of 10^4–10^5 L mol^{-1}, which agreed with the common affinities of drugs for protein [27]. The number of binding sites for W_3 (or **W_4**) was about 1.0, which indicated that one binding site formed between **W_3** (or **W_4**) and FTO. Quantitative consideration of the data presented here provides a measure of the strength of FTO−**W_3** (or **W_4**) associations. Fluorescence titrations of FTO with **W_3** suggest primary sites with K_a on the order of 10^5 L mol^{-1}. For **W_4**, the value of K_a was on the order of 10^4 L mol^{-1}. The binding constant values show that the strength of interactions for **W_3** is stronger than the interactions for **W_4**.

Binding Modes

The intermolecular acting forces between small molecular substrates and biomolecule may be hydrogen bonds, van der Waals interactions, electrostatic interactions, hydrophobic force, etc. The thermodynamic parameters of the reaction are important evidence for confirming the binding force. If the temperature varies in a small range, the enthalpy change is regarded as a constant. The van't Hoff relationship is based on the assumption of a nearly constant enthalpy change [28]. To characterize the forces involved in the **W_3** (or **W_4**)–FTO interaction, the values of enthalpy change (ΔH), entropy

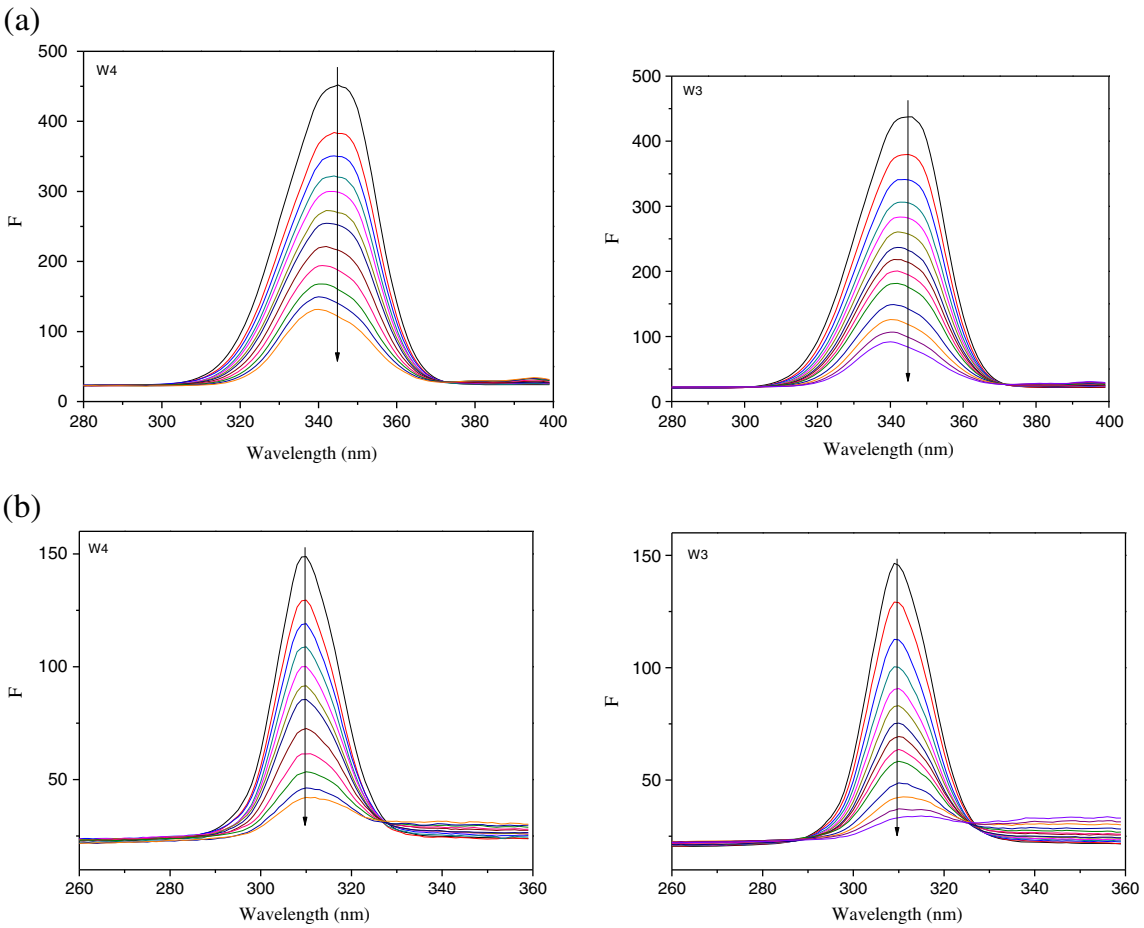

Fig. 7 The synchronous fluorescence spectra upon addition of W_3 (or W_4). **a** $\Delta\lambda$=60, **b** $\Delta\lambda$=15. Tris–HCl pH=7.40; FTO 1.5×10^{-5} mol·L^{-1}. The concentration of W_3 (or W_4) is 1.0×10^{-5}, 2.0×10^{-5}, 3.0×10^{-5}, 4.0×10^{-5}, 5.0×10^{-5}, 6.0×10^{-5}, 7.0×10^{-5}, 8.0×10^{-5}, 1.0×10^{-4}, 1.3×10^{-4}, 1.5×10^{-4} and 1.8×10^{-4} mol L^{-1} respectively (From *top* to *bottom*)

change (ΔS) and the free-energy change (ΔG) were evaluated from the van't Hoff plot and thermodynamic equations [29] and were listed in Table 3.

$$\ln K_a = -\frac{\Delta \mathrm{H}}{RT} + \frac{\Delta \mathrm{S}}{R} \tag{3}$$

$$\Delta \mathrm{G} = \Delta \mathrm{G} - T\Delta S \tag{4}$$

where K_a is the binding constant at corresponding temperature, R is the gas constant (R=8.314 J·moL^{-1}·K^{-1}), ΔH and ΔS are calculated from the slope and the intercept of this linear plot between lnK_a and 1/T based on Eq. (3). The free energy change (ΔG) could be calculated by the Eq. (4).

As shown in Table 3, the negative ΔG means that the binding process was spontaneous. Both ΔH and ΔS values of the interaction of $\mathbf{W_3}$ (or $\mathbf{W_4}$) with FTO are positive. According to the views of Ross and Subramanian [30], hydrophobic interaction is characterized by a positive value of ΔS and a positive ΔH value. Therefore, it can be deduced that the acting forces are mainly hydrophobic interactions between the interactions of FTO with $\mathbf{W_3}$ (or $\mathbf{W_4}$) [31, 32].

Synchronous Fluorescence

Alteration in the microenvironment around the tyrosine (Tyr) and tryptophan (Trp) in the structure of FTO upon $\mathbf{W_3}$ (or $\mathbf{W_4}$) binding was elucidated by synchronous fluorescence spectra (Fig. 7, (a) for $\Delta\lambda$ =60 nm and (b) for $\Delta\lambda$=15 nm). Figure 7 show the effect of increasing concentrations of $\mathbf{W_3}$ (or $\mathbf{W_4}$) on the synchronous fluorescence spectra of FTO at the $\Delta\lambda$ value of 15 and 60 nm, respectively. While no obvious change in the emission maxima (310 nm) was observed upon addition of $\mathbf{W_3}$ (or $\mathbf{W_4}$) when $\Delta\lambda$ was 15 nm, synchronous fluorescence spectra obtained with $\Delta\lambda$=60 nm showed a blue shift from 348 to 340 nm upon $\mathbf{W_3}$ (or $\mathbf{W_4}$) addition. The observed blue shift signified a transition of the Trp residues from a polar to a less polar environment [6]. Results suggested that binding of $\mathbf{W_3}$ (or $\mathbf{W_4}$) to FTO had little effect on the microenvironment around Tyr residues but was sufficient to perturb the environment in the vicinity of the lone Trp residue from polar to slightly nonpolar.

Three-Dimensional Fluorescence Spectra

The three-dimensional fluorescence spectra are a rising fluorescence analysis technique. The excitation wavelength, the emission wavelength and the fluorescence intensity can be used as the axes in order to investigate the synthetically information of the samples [33]. Figure 8 presented the representative three-dimensional fluorescence spectra of FTO (a) and FTO–$\mathbf{W_3}$ (b). Results showed that three-dimensional fluorescence spectra of FTO and FTO–$\mathbf{W_3}$ were different obviously. The intensity of one peaks decreased obviously. Similar results were obtained for $\mathbf{W_4}$. The phenomena revealed that the

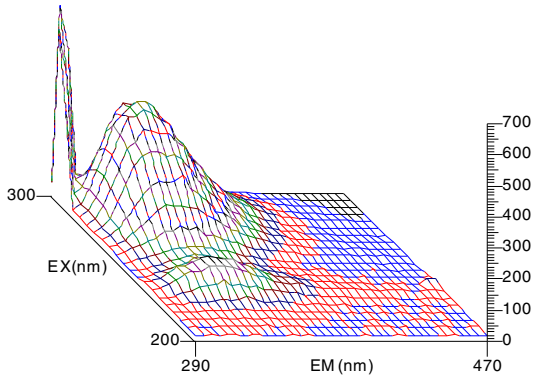

(a) FTO

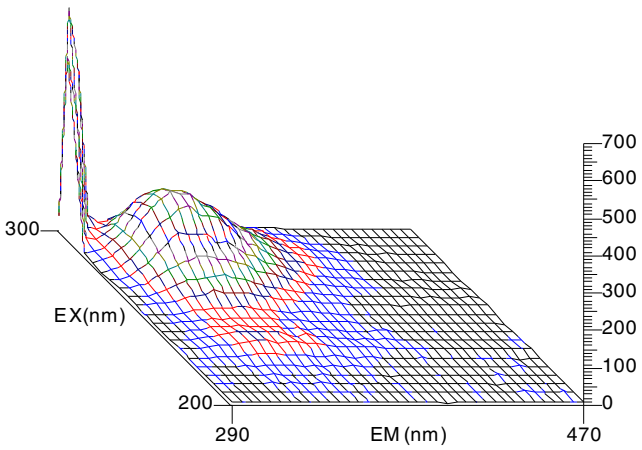

(b) FTO+W_3

Fig. 8 The three-dimensional fluorescence spectra of FTO (**a**), FTO–$\mathbf{W_3}$ (**b**). The concentration of FTO is 1.5×10^{-5} mol/L and the concentration of $\mathbf{W_3}$ is 8.0×10^{-5} mol/L

interaction of FTO–$\mathbf{W_3}$ (or $\mathbf{W_4}$) induced some microenvironmental and conformational changes in FTO [34].

Comparison Between $\mathbf{W_3}$ and $\mathbf{W_4}$

There is a similar main structure in the molecular of $\mathbf{W_3}$ and $\mathbf{W_4}$. The difference between $\mathbf{W_3}$ and $\mathbf{W_4}$ is the size of the ring. The binding constant for $\mathbf{W_3}$ was larger. Analyzing from the binding constants for $\mathbf{W_3}$ and $\mathbf{W_4}$, $\mathbf{W_3} > \mathbf{W_4}$ may be explained by the different between the ternary ring and four-member ring. $\mathbf{W_3}$ showed a stronger quenching effect with FTO. The interaction with FTO was enhanced by the ternary ring. The reason may be that the ternary ring showed smaller steric hindrance in the interaction.

Conclusions

In summary, the interactions between FTO and $\mathbf{W_3}$ or $\mathbf{W_4}$ were studied. The influence of molecular structure on the

binding aspects has been investigated. The binding study of drugs to proteins is important in pharmacy, pharmacology and biochemistry and so on.

Fluorescence spectroscopy provides qualitative and quantitative information about the interaction between FTO and $\mathbf{W_3}$ or $\mathbf{W_4}$. Our results showed that the intrinsic fluorescence of FTO was quenched through static quenching mechanism. The binding reaction mainly involved hydrophobic interaction as revealed by thermodynamic parameters. The microenvironment of Trp residues of FTO were disturbed by the binding of $\mathbf{W_3}$ or $\mathbf{W_4}$ to FTO as analyzed by intrinsic and synchronous fluorescence. $\mathbf{W_3}$ and $\mathbf{W_4}$ displayed different binding ability. Thermodynamic results also showed that the $\mathbf{W_3}$ show stronger quenching ability than $\mathbf{W_4}$. This study may provide valuable information about the inhibitors of FTO.

Acknowledgments We are grateful to the National Natural Science Foundation of China (#81330075) for financial support.

References

1. Tung YC, Yeo GS, O'Rahilly S, Coll AP (2014) Cell Metab 20(5): 710
2. Chen B, Ye F, Yu L, Jia G, Huang X, Zhang X, Peng S, Chen K, Wang M, Gong S, Zhang R, Yin J, Li H, Yang Y, Liu H, Zhang J, Zhang H, Zhang A, Jiang H, Luo C, Yang CG (2012) J Am Chem Soc 134:17963
3. Zheng G, Cox T, Tribbey L, Wang GZ, Iacoban P, Booher ME, Gabriel GJ, Zhou L, Bae N, Rowles J, He C, Olsen MJ (2014) ACS Chem Neurosci 5:658
4. Aik WS, Demetriades M, Hamdan MKK, Bagg EAL, Yeoh KK, Lejeune C, Zhang Z, McDonough MA, Schofield CJ (2013) J Med Chem 56:3680
5. A binding site for FTO inhibitors ($\mathbf{W_4}$) was established by the crystal structure of FTO by the coauthors, Wu He, Qinghua Yang and Ruiyong Wang. The identification of the new binding site offers new opportunities for further development of selective and potent inhibitors of FTO, which is expected to provide information concerning novel therapeutic targets for treatment of obesity or obesity-associated diseases. The detailed biological work will be published by Wu He, Qinghua Yang and Ruiyong Wang in due course.
6. Feroz S, Mohamad S, Bujang N, Malek SN, Tayyab S (2012) J Agric Food Chem 60(23):5899
7. Messina PV, Prieto G, Ruso JM, Sarmiento F (2005) J Phys Chem B 109(32):15566
8. Sabin J, Prieto G, Gonzalez-Perez A, Ruso JM, Sarmiento F (2006) Biomacromolecules 7(1):176
9. Lissi E, Abuin E, Lanio ME, Alvarez C (2002) J Biochem Biophys Methods 50(2):261
10. De S, Girigoswami A, Das S (2005) J Colloid Interface Sci 285(2): 562
11. Messina P, Prieto G, Dodero V, Ruso JM, Schulz P, Sarmiento F (2005) Biopolymers 79(6):300
12. MacManus-Spencer LA, Tse ML, Hebert PC, Bischel HN, Luthy RG (2010) Anal Chem 82(3):974
13. Han Z, Niu T, Chang J, Lei X, Zhao M, Wang Q, Cheng W, Wang J, Feng Y, Chai J (2010) Nature 464:1205
14. Peters T Jr (1985) Adv Protein Chem 37:161
15. Wang R, Kang X, Wang R, Wang R, Dou H, Wu J, Song C, Chang J (2013) J Lumin 138:258
16. Wang XR, Xie XY, Ren CL (2011) Food Chem 127(2):705
17. Gao XY, Tang YC, Rong WQ, Zhang X, Zhao W, Zi Y (2011) Am J Anal Chem 2:250
18. Zeng XD, Zhu L, Zhang FS, Feng LY (2013) J Lumin 138:44
19. Bakkialakshmi S, Chandrakala D (2012) Spectrochim Acta A 88:2
20. Wang R, Chai Y, Wang R, Zhang L, Wu J, Chang J (2012) Spectrochim Acta A 96:324
21. Lakwiocz JR (2006) Principles of fluorescence spectroscopy, 3rd edn. Plenum Press, New York, pp 443–516
22. Hegdge AH, Sandhya B, Seetharamappa J (2011) Mol Biol Rep 38: 4921
23. Ware WR (1962) J Phys Chem 66:455
24. Tong JQ, Tian FF, Liu Y, Jiang FL (2014) RSC Adv 4:59686
25. Hazra S, Kumar GS (2014) J Phys Chem B 118:3771
26. Hu Y, Liu Y, Wang J, Xiao X, Qu S (2004) J Pharm Biomed Anal 36(4):915
27. Seedher N, Agarwal P (2010) J Lumin 130(10):1841
28. Cheng HX, Liu H, Bao W, Zou GL (2011) J Photochem Photobiol B 105:126
29. Zhao HW, Ge M, Zhang ZX, Wang W, Wu G (2006) Spectrochim Acta A 65:811
30. Ross PD, Subramanian S (1981) Biochemistry 20:3096
31. Zhang YZ, Dai J, Zhang XP, Yang X, Liu Y (2008) J Mol Struct 888:152
32. Cui F, Yan Y, Zhang Q, Yao X, Qu G, Lu Y (2009) Spectrochim Acta A 74:964
33. Li Z, Li Z, Yang L, Xie Y, Shi J, Wang R, Chang J (2015) J Fluoresc 25:451
34. Wang R, Wang X, Li Z, Xie Y, Yang L, Shi J, Chang J (2014) Spectrochim Acta A 132:786